

RESPONSE OF THE TROPICAL ATMOSPHERE  
TO CONVECTIVE CLOUD CLUSTERS

Wayne H. Schubert  
Paul E. Ciesielski

Department of Atmospheric Science, Colorado State University  
Fort Collins, Colorado, USA

James J. Hack

IBM Thomas J. Watson Research Center  
Yorktown Heights, New York, USA

1. INTRODUCTION

How does the tropical atmosphere dynamically respond to the release of latent heat in clusters of convective clouds? This depends on several factors, including: (1) the latitude of the cluster, (2) the horizontal scale of the cluster; (3) the time scale of the cluster; (4) the "static" and "inertial" stabilities of the flow in which the cluster is imbedded. The first three factors can be studied using linear models on an  $f$ -plane (e.g. Schubert et al., 1980) or an equatorial  $\beta$ -plane (e.g. Silva Dias et al., 1983). The last factor is essentially nonlinear because the static and inertial stabilities (and hence also the response) change as the flow field evolves. In particular, the pressure fall and the tangential wind acceleration produced by a heat source imbedded in a strong vortex can be much larger than the corresponding changes produced by the same heat source in a weak vortex (Schubert and Hack, 1982). In order to understand the crucial nature of this nonlinear effect in hurricane development, let us consider the following model experiments performed with two simplified versions of the axisymmetric, 18 level,  $\sigma$  coordinate hurricane model described by Hack and Schubert (1980).

The axisymmetric,  $f$ -plane, inviscid response to the specified heat source  $Q(r,z,t)$  is determined by the system of equations<sup>1</sup>

$$\frac{\partial u}{\partial t} + u \frac{\partial u}{\partial r} + w \frac{\partial u}{\partial z} - (f + \frac{v}{r})v + \frac{\partial \phi}{\partial r} = 0, \quad (1.1)$$

$$\frac{\partial v}{\partial t} + u \frac{\partial v}{\partial r} + w \frac{\partial v}{\partial z} + (f + \frac{v}{r})u = 0, \quad (1.2)$$

$$\frac{\partial \phi}{\partial z} = \frac{g}{\theta_0} \theta, \quad (1.3)$$

---

<sup>1</sup> Although the numerical results presented in this section were obtained from a  $\sigma$ -coordinate model, for convenience of later discussion we present the governing equations in pseudo-height coordinate form.

$$\frac{\partial ru}{r\partial r} + \frac{\partial \rho w}{\rho \partial z} = 0, \quad (1.4)$$

$$\frac{\partial \ln \theta}{\partial t} + u \frac{\partial \ln \theta}{\partial r} + w \frac{\partial \ln \theta}{\partial z} = \frac{Q}{c_p T}, \quad (1.5)$$

where  $z = [1 - (\frac{p}{p_0})^{\kappa}] \frac{c_p \theta}{g}$  is the pseudo-height,  $\rho(z)$  the known pseudo-density,  $u$ ,  $v$ ,  $w$  the radial, tangential and vertical components of velocity,  $\theta$  the potential temperature, and  $\phi$  the geopotential. We shall refer to the system (1.1)-(1.5) as the nonlinear model. If all the underlined terms in (1.1)-(1.5) are neglected and  $\frac{\partial \ln \theta}{\partial z}$  is replaced by a specified mean tropical atmosphere profile  $\frac{\partial \ln \bar{\theta}}{\partial z}$ , the resulting system will be referred to as the linear model. We wish to illustrate the different responses produced by the linear and nonlinear models. As for the specified heat source  $Q$ , let us assume that

$$q(r,z,t) = \begin{cases} \hat{q}(z) e^{-r^2/a^2} & t > 0 \\ 0 & t < 0 \end{cases} \quad (1.6)$$

where  $a=150$  km. The vertical structure  $\hat{q}$  is chosen such that the horizontally averaged  $q$  inside 250 km matches the vertical profile of apparent heat source given by Yanai et al. (1973). The instantaneous switch-on of the heating at  $t=0$  excites some transient gravity wave activity, but this activity leaves the computational domain because of the radiation boundary condition (Hack and Schubert, 1981).

In Figs. 1 and 2 we present the time evolution of the central surface pressure, the maximum tangential wind, and the radius of maximum tangential wind for the linear (dashed lines) and the nonlinear (solid lines) models. The linear model produces a vortex with a fixed radius of maximum wind ( $\sim 160$  km), a central surface pressure tendency of 0.75 mb/day, and a maximum tangential wind change of about  $3\text{ms}^{-1}/\text{day}$ . The nonlinear model produces a vortex which begins to deviate significantly from the linear model vortex after 24-48 hours. As the radius of maximum wind moves inward, the central surface pressure and the maximum tangential wind begin to change more and more rapidly. Near the end of the five-day integration the surface pressure tendency in the nonlinear model is about twenty times that in the linear model while the maximum tangential wind change is three times the linear rate. In general the nonlinear model results are much more reminiscent of the type of behavior observed in developing hurricanes and typhoons. In the remainder of this paper we shall try to understand the nonlinear behavior from the viewpoint of the Eliassen balanced vortex model.

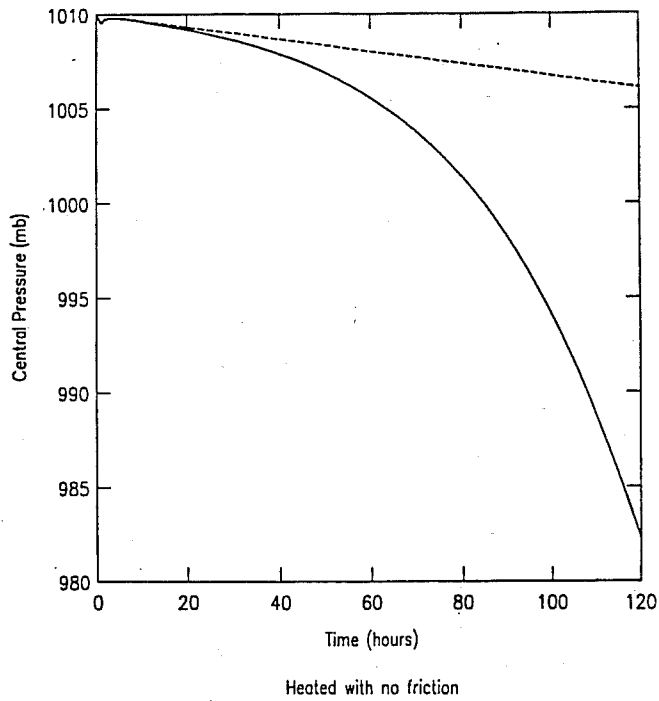


Fig. 1. Time evolution of the central surface pressure.

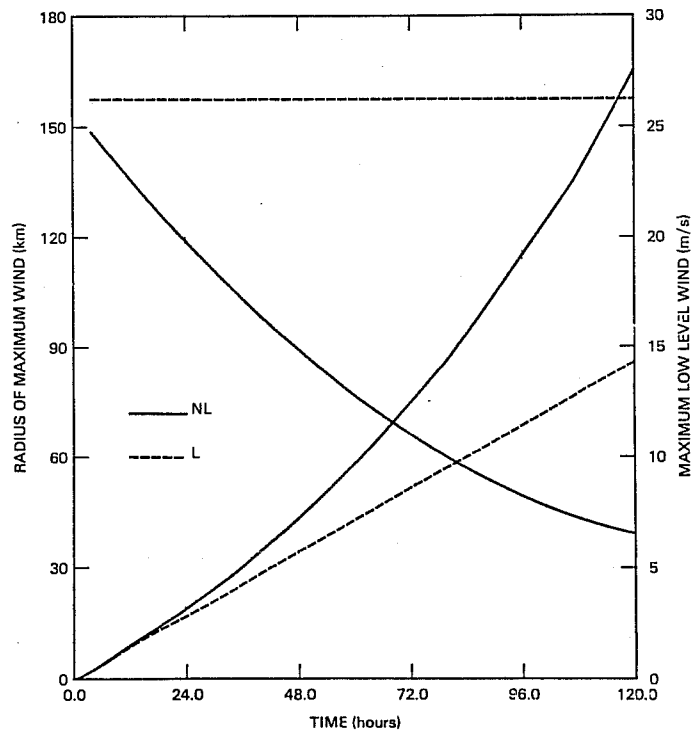


Fig. 2. Time evolution of the maximum tangential wind (scale on right) and the radius of maximum tangential wind (scale on left) for the linear (dashed lines) and nonlinear (solid lines) models.

## 2. BALANCED VORTEX MODEL

We now consider axisymmetric flows which are forced by heat sources with slow time variations. The flow is then always close to a state of gradient balance, and (1.1) can be approximated by

$$(f + \frac{v}{r})v = \frac{\partial \phi}{\partial r}.$$

Above the boundary layer the absolute angular momentum per unit mass  $\frac{fR^2}{2} = rv + \frac{fr^2}{2}$  is conserved. We call  $R$  the potential radius, i.e. the radius to which a parcel must be moved (conserving absolute angular momentum) in order to change its tangential component of velocity to zero. We can now write the governing equations for the flow above the boundary layer as (2.1)-(2.5), which are given on the left side of Table 1. The effect of friction is crudely incorporated through the pumping relation (2.6), which serves as the lower boundary condition on (2.1)-(2.5). Here  $\zeta = f \frac{\partial}{\partial r} (\frac{R^2}{2})$  is the vertical component of absolute vorticity, and subscript zero denotes a top of the boundary layer (i.e.  $z=0$ ) value. A more extensive discussion of (2.1)-(2.6), along with the associated pseudo-conservation relations for vector vorticity, potential vorticity and energy, is given in Schubert and Hack (1983).

Table 1.

$\frac{1}{4} f^2 \frac{(R^4 - r^4)}{r^3} = \frac{\partial \phi}{\partial r}$ (2.1)	$\frac{1}{2} f^2 \frac{(R^2 - r^2)}{r^2} = \frac{\partial \phi}{\partial R}$ (2.7)
$\frac{\partial}{\partial t} (\frac{R^2}{2}) + u \frac{\partial}{\partial r} (\frac{R^2}{2}) + w \frac{\partial}{\partial z} (\frac{R^2}{2}) = 0$ (2.2)	$\frac{\partial}{\partial T} (\frac{r^2}{2}) - Ru^* = 0$ (2.8)
$\frac{g}{\theta_0} \theta = \frac{\partial \phi}{\partial z}$ (2.3)	$\frac{g}{\theta_0} \theta = \frac{\partial \phi}{\partial Z}$ (2.9)
$\frac{\partial ru}{\partial r} + \frac{\partial \rho w}{\rho \partial z} = 0$ (2.4)	$\frac{\partial Ru^*}{\partial R} + \frac{\partial \rho w^*}{\rho \partial Z} = 0$ (2.10)
$\frac{\partial \theta}{\partial t} + u \frac{\partial \theta}{\partial r} + w \frac{\partial \theta}{\partial z} = Q$ (2.5)	$\frac{\partial \theta}{\partial T} + \frac{\theta_0}{g} q \rho w^* = Q$ (2.11)
$w_0 = \frac{\partial}{\partial r} \left\{ \frac{f}{\zeta_0} c_D  v_0  \frac{1}{2} (R_0^2 - r^2) \right\}$ (2.6)	$w_0^* = \frac{\partial}{\partial R} \left\{ \frac{f}{\zeta_0} c_D  v_0  \frac{1}{2} (R^2 - r_0^2) \right\}$ (2.12)

We now wish to transform (2.1)-(2.6) from  $(r, z, t)$  space to  $(R, Z, T)$  space, where  $Z=z$  and  $T=t$ . The upper case symbols for pseudo-height and time are introduced to distinguish derivatives at constant radius ( $\frac{\partial}{\partial Z}$  and  $\frac{\partial}{\partial T}$ ) from derivatives at constant potential radius ( $\frac{\partial}{\partial r}$  and  $\frac{\partial}{\partial t}$ ). In analogy with semi-geostrophic theory (Hoskins, 1975; Hoskins and Draghici, 1977) we introduce the potential function

$$\bar{\phi} = \phi + \frac{1}{2} v^2 = \phi + \frac{1}{8} f^2 \frac{(R^2 - r^2)^2}{r^2},$$

and the new transverse circulation components

$$Ru^* = r(u - w \frac{\partial r}{\partial Z}),$$

$$w^* = \frac{f}{\zeta} w.$$

Then, as discussed more fully in Schubert and Hack (1983), our governing system (2.1)-(2.6) becomes (2.7)-(2.12), which is shown on the right of Table 1 for easy comparison. Here the vertical component of absolute vorticity  $\zeta$  is given by  $\frac{f}{\zeta} = \frac{\partial}{R\partial R} (\frac{r^2}{2})$  and the potential vorticity  $q$  by  $\rho q = \frac{\zeta}{f} \frac{g}{\theta_0} \frac{\partial \theta}{\partial Z}$ . In comparing the two columns of Table 1 we note that (2.7)-(2.12) represent a considerable simplification over (2.1)-(2.6) since the mathematical forms of the hydrostatic, continuity and boundary layer pumping equations have remained essentially unchanged while the gradient, tangential momentum and thermodynamic equations have all been simplified.

### 3. DUAL FORMS OF THE TRANSFORMED MODEL

If we use the gradient wind equation (2.7) in (2.8) and the hydrostatic equation (2.9) in (2.11) we obtain

$$\Phi_{RT} + s\rho u^* = 0, \quad (3.1)$$

$$\Phi_{ZT} + q\rho w^* = \frac{g}{\theta_0} Q, \quad (3.2)$$

where the inertial stability  $s$  is given by  $\rho s = f^2 \frac{R^4}{r^4}$ . There are now two ways to proceed. The first is similar to the method discussed by Schubert and Hack (1983) and consists of eliminating  $\Phi_T$  between (3.1) and (3.2) to obtain the transverse circulation equation. The second consists of using the continuity equation (2.10) to eliminate  $u^*$  and  $w^*$  between (3.1) and (3.2), which results in the tendency equation for  $\Phi$ . We now discuss each of these approaches.

#### a. Transverse circulation form

Defining the streamfunction  $\psi^*$  such that

$$(\rho u^*, \rho w^*) = \left( -\frac{\partial \psi^*}{\partial Z}, \frac{\partial R \psi^*}{R \partial R} \right), \quad (3.3)$$

then subtracting  $\frac{\partial}{\partial Z}$  of (3.1) from  $\frac{\partial}{\partial R}$  of (3.2) we obtain the transverse circulation equation

$$\left\{ \begin{array}{l} \frac{\partial}{\partial R} \left( q \frac{\partial R \psi^*}{R \partial R} \right) + \frac{\partial}{\partial Z} \left( s \frac{\partial \psi^*}{\partial Z} \right) = \frac{g}{\theta_0} \frac{\partial Q}{\partial R} \\ \psi^*(0, Z) = \psi^*(R, Z_T) = 0, R \psi^* \rightarrow 0 \text{ as } R \rightarrow \infty, \\ R \psi^*(R, 0) = \frac{f}{\zeta_0} \rho_0 c_D |v_0| \frac{1}{2} (R^2 - r_0^2) \end{array} \right. \quad (3.4)$$

b. Potential tendency form

Multiplying (3.1) by  $\frac{R}{s}$  and then taking  $\frac{\partial}{R \partial R}$ , multiplying (3.2) by  $\frac{1}{q}$  and then taking  $\frac{\partial}{\partial Z}$ , and finally combining these results with the aid of the continuity equation (2.10) we obtain

$$\left\{ \begin{array}{l} \frac{\partial}{R \partial R} \left( \frac{R}{s} \frac{\partial \Phi_T}{\partial R} \right) + \frac{\partial}{\partial Z} \left( \frac{1}{q} \frac{\partial \Phi_T}{\partial Z} \right) = \frac{g}{\theta_0} \frac{\partial}{\partial Z} \left( \frac{Q}{q} \right) \\ \frac{\partial \Phi_T}{\partial R} = 0 \text{ at } R = 0, \frac{\partial \Phi_T}{\partial R} \rightarrow 0 \text{ as } R \rightarrow \infty, \\ \frac{\partial \Phi_T}{\partial Z} = \frac{g}{\theta_0} Q - \left\{ \begin{array}{ll} 0 & Z = Z_T \\ q_0 \rho_0 w_0^* & Z = 0 \end{array} \right\} \end{array} \right. \quad (3.5)$$

In the case where  $Q$  vanishes at the top and bottom boundaries and  $w_0^* = 0$ , the solution  $\Phi_T$  can be determined only to within an arbitrary additive constant. An additional global condition can then be imposed to insure uniqueness (e.g. Courant and Hilbert, Vol. I, pages 248-249).

c. Summary of the dual forms

The dual forms of the transformed Eliassen balanced vortex model are summarized in Table 2. The left column gives the transverse circulation form and the right column the potential tendency form. Roughly speaking, a computer program makes use of each equation in the order given. The important point for present purposes is that the coefficients  $q$  and  $s$  in (3.10) and (3.19) change as the vortex evolves. Thus, the response to a given  $Q$  also changes.

In passing we note the following interesting mathematical difference between the two forms of the balanced model. Because the transverse circulation form (3.6)-(3.13) uses the thermal wind equation (3.6) to compute  $r$  from  $\theta$ , a reference level value of  $r$  must be known. This is determined by (3.13). In contrast the

potential tendency form (3.14)-(3.19) uses the gradient wind equation (3.14) to compute  $r$  from  $\phi$ , and (3.13) is not needed. Apparently, the price of this simplification is that the Dirichlet boundary conditions of (3.10) are replaced by the Neumann conditions of (3.19).

Table 2.

$-f^2 \frac{R^3}{r^3} \frac{\partial r}{\partial Z} = \frac{g}{\theta_0} \frac{\partial \theta}{\partial R} \quad (3.6)$	$\frac{1}{2} f^2 \frac{R(R^2 - r^2)}{r^2} = \frac{\partial \phi}{\partial R} \quad (3.14)$
$\frac{f}{c} = \frac{\partial}{\partial R} \left( \frac{r^2}{2} \right) \quad (3.7)$	$\frac{g}{\theta_0} \theta = \frac{\partial \phi}{\partial Z} \quad (3.15)$
$\rho q = \frac{c}{f} \frac{g}{\theta_0} \frac{\partial \theta}{\partial Z} \quad (3.8)$	$\frac{f}{c} = \frac{\partial}{\partial R} \left( \frac{r^2}{2} \right) \quad (3.16)$
$\rho s = f^2 \frac{R^4}{r^4} \quad (3.9)$	$\rho q = \frac{c}{f} \frac{g}{\theta_0} \frac{\partial \theta}{\partial Z} \quad (3.17)$
$\left\{ \begin{array}{l} \frac{\partial}{\partial R} \left( q \frac{\partial R \psi^*}{\partial R} \right) + \frac{\partial}{\partial Z} \left( s \frac{\partial \psi^*}{\partial Z} \right) = \frac{g}{\theta_0} \frac{\partial Q}{\partial R} \\ \text{B.C. } \psi^*(0, Z) = \psi^*(R, Z_T) = 0, \quad R \psi^* \rightarrow 0 \text{ as } R \rightarrow \infty, \\ R \psi^*(R, 0) = \frac{f}{c_0} \rho_0 c_D  v_0  \frac{1}{2} (R^2 - r_0^2) \end{array} \right. \quad (3.10)$	$\left\{ \begin{array}{l} \frac{\partial}{\partial R} \left( \frac{R}{s} \frac{\partial \phi_T}{\partial R} \right) + \frac{\partial}{\partial Z} \left( \frac{1}{q} \frac{\partial \phi_T}{\partial Z} \right) = \frac{g}{\theta_0} \frac{\partial}{\partial Z} \left( \frac{Q}{q} \right) \\ \text{B.C. } \frac{\partial \phi_T}{\partial R} = 0 \text{ at } R=0, \quad \frac{\partial \phi_T}{\partial R} \rightarrow 0 \text{ as } R \rightarrow \infty \\ \frac{\partial \phi_T}{\partial Z} = \frac{g}{\theta_0} Q - \left\{ \begin{array}{l} 0 \quad Z = Z_T \\ q_0 \rho_0 w_0^* \quad Z = 0 \end{array} \right. \end{array} \right. \quad (3.19)$
$(\rho u^*, \rho w^*) = \left( -\frac{\partial \psi^*}{\partial Z}, \frac{\partial R \psi^*}{\partial R} \right) \quad (3.11)$	
$\frac{\partial \theta}{\partial T} + \frac{\theta}{g} \rho q w^* = Q \quad (3.12)$	
$f^2 \frac{R^3}{r_0^3} \frac{\partial r_0}{\partial T} - \rho_0 s_0 u_0^* = 0 \quad (3.13)$	

#### 4. SIMPLE ANALYTICAL SOLUTION

We consider the idealized situation in which  $q$  and  $s$  are constants and the heating is given by

$$Q(R, Z) = \begin{cases} \hat{Q} \sin \left( \frac{\pi Z}{Z_T} \right) & R < \hat{R} \\ 0 & R > \hat{R} \end{cases} \quad (4.1)$$

where  $\hat{Q}$  is a constant. If all this heating were to appear locally as a temperature change (i.e. if  $w^*$  in (3.2) were zero), then the resulting potential tendency would be

$$\hat{\phi}_T(R, Z) = \begin{cases} -\frac{g Z_T}{\theta_0 \pi} \hat{Q} \cos \left( \frac{\pi Z}{Z_T} \right) & R < \hat{R} \\ 0 & R > \hat{R} \end{cases} \quad (4.2)$$

In reality, of course,  $w^*$  is not zero, and the actual potential tendency is found by substituting (4.1) into (3.5) and solving the resulting equation by the method

of separation of variables. The radial structure equation is a modified Bessel equation of order zero. It is inhomogeneous in the region  $0 < R < \hat{R}$  and homogeneous in the region  $\hat{R} < R < \infty$ . Once solutions are found in these two regions they must be matched across  $\hat{R}$  in such a way that both  $\Phi_T$  and  $\frac{\partial \Phi_T}{\partial R}$  are continuous. The result is

$$\frac{\Phi_T(R,Z)}{|\hat{\Phi}_T(0,0)|} = \begin{cases} \mu \hat{R} K_1(\mu \hat{R}) I_0(\mu R) - 1 & R < \hat{R} \\ -\mu \hat{R} I_1(\mu \hat{R}) K_0(\mu R) & R > \hat{R} \end{cases} \cos\left(\frac{\pi Z}{Z_T}\right), \quad (4.3)$$

where  $\mu^{-1} = \left(\frac{q}{s}\right)^{\frac{1}{2}} \frac{Z_T}{\pi}$  is the generalized Rossby radius.

Using (4.3) we have computed  $\Phi_T(R,Z)/|\hat{\Phi}_T(0,0)|$  at the top of the boundary layer ( $Z=0$ ) for the three cases  $\mu \hat{R} = 0.2, 1, 5$ . These results are displayed in Fig. 3. For comparison we have also included  $\hat{\Phi}_T(R,Z)/|\hat{\Phi}_T(0,0)|$  at  $Z=0$ . This rectangular well pattern represents the normalized tendency which would occur if all the heating appeared as a local thickness change (i.e. if  $w^*$  were zero). Fig. 3 reveals the enhanced response which occurs as  $\mu$  increases for fixed  $\hat{R}$ .

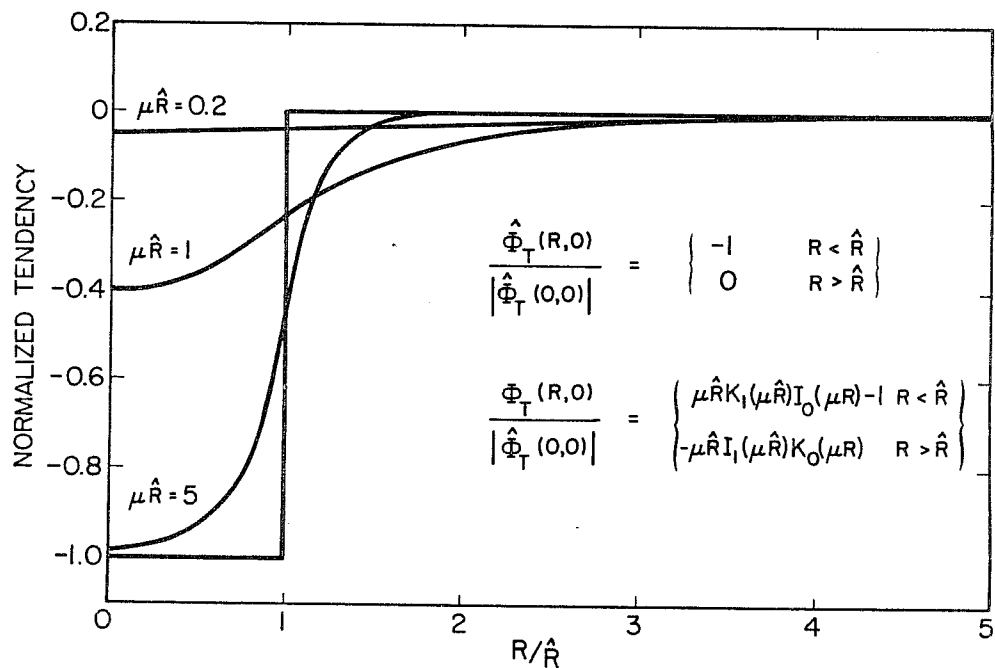


Fig. 3. The three smooth curves are the normalized potential tendency  $\Phi_T(R,0)/|\hat{\Phi}_T(0,0)|$  for three different values of  $\mu \hat{R}$ . For comparison the rectangular pattern  $\hat{\Phi}_T(R,0)/|\hat{\Phi}_T(0,0)|$  is also shown.

The results shown in Fig. 3 have been obtained under the assumption of constant  $q$  and  $s$ . As shown in Schubert and Hack (1983) nature's tropical cyclones have considerable radial and vertical variation of  $q$  and  $s$ . However, there is a tendency for the local value of  $\mu$  to become large in the inner region where  $Q$  is large. This apparently explains the results obtained in Figs. 1 and 2.



It is interesting to note that tropical cyclone development is primarily a nonlinear process and is similar in some respects to frontogenesis, where very large (infinite!) vorticity is produced in a finite time. Two important differences are that frontogenesis is forced by a larger scale flow such as a deformation field while the tropical cyclone is forced by the release of latent heat, and that curvature effects can be neglected in most frontogenesis studies but are important for the tropical cyclone.

## 5. ENERGETICS AND EFFICIENCY

From the balanced version of (1.1)-(1.5) and the boundary condition (2.6) we can derive the energy equations

$$\frac{dP}{dt} = H - C, \quad (5.1)$$

$$\frac{dK}{dt} = C - D, \quad (5.2)$$

where

$$P = \iiint c_p T \rho r dr dz, \quad (5.3)$$

$$K = \iiint \frac{1}{2} v^2 \rho r dr dz, \quad (5.4)$$

$$H = \iiint Q \rho r dr dz, \quad (5.5)$$

$$C = \iiint \frac{g}{\theta_0} w \theta \rho r dr dz, \quad (5.6)$$

$$D = \int c_D |v_0| v_0^2 \rho_0 r dr. \quad (5.7)$$

The radial integrals in (5.3)-(5.7) extend from  $r$  equals zero to infinity and the vertical integrals from  $z$  equals zero to  $z_T$ . Hence,  $P$  and  $K$  denote the total potential and kinetic energies of the atmosphere,  $H$  the total heating,  $C$  the rate of conversion of total potential energy into kinetic energy, and  $D$  the frictional dissipation.

Using the fact that  $r dr dz = \frac{f}{z} R dR dZ$  we can write (5.6) as

$$C = \iiint \frac{g}{\theta_0} w^* \theta \rho R dR dZ. \quad (5.8)$$

Following Eliassen (1952) we shall now express  $C$  in terms of the heating  $Q$ . For simplicity we assume the flow is frictionless ( $c_D=0$ ). Using (3.11) and integrating

by parts we can rewrite (5.8) as

$$C = - \iint \frac{g}{\theta_0} \frac{\partial \theta}{\partial R} \psi^* R dR dZ . \quad (5.9)$$

Let us define  $\Psi^*$  as the solution of

$$\left\{ \begin{array}{l} \mathcal{L}\Psi^* = \frac{\partial}{\partial R} \left( q \frac{\partial R\Psi^*}{R\partial R} \right) + \frac{\partial}{\partial Z} \left( s \frac{\partial \Psi^*}{\partial Z} \right) = \frac{g}{\theta_0} \frac{\partial \theta}{\partial R} \\ \text{B.C. } \Psi^*(0,Z) = \Psi^*(R,Z_T) = \Psi^*(R,0) = 0 , \\ R\Psi^* \rightarrow 0 \text{ as } R \rightarrow \infty \end{array} \right. \quad (5.10)$$

so that (5.9) becomes

$$C = - \iint \psi^* \mathcal{L} \Psi^* R dR dZ = - \iint \Psi^* \mathcal{L} \psi^* R dR dZ . \quad (5.11)$$

The last step (i.e. the self-adjoint property) can be proved by integrating by parts twice in both  $R$  and  $Z$ , and using the boundary conditions on  $\psi^*$  and  $\Psi^*$ . Finally, the right hand side of (3.10) can be substituted for  $\mathcal{L}\psi^*$ , after which an integration by parts yields

$$C = \frac{g}{\theta_0} \iint \frac{\partial R\Psi^*}{R\partial R} Q R dR dZ . \quad (5.12)$$

This way of expressing  $C$  allows us to argue as follows. Suppose we know the structure of a vortex at a given time. We then know the coefficients  $q$  and  $s$  and the right hand side  $\frac{g}{\theta_0} \frac{\partial \theta}{\partial R}$  in (5.10). We can solve for  $\Psi^*$  and construct the field  $\frac{\partial R\Psi^*}{R\partial R}$ . Then, according to (5.12), we can determine if the heating field  $Q$  is distributed so as to give an efficient conversion of total potential energy to kinetic energy. Our hypothesis is that certain tropical disturbances possess combinations of vortex structure and heating which are very efficient, and these are the ones that become hurricanes and typhoons<sup>1</sup>.

In Fig. 4 we show a field of  $v(R,Z)$  patterned after the large typhoon composite data of R. Merrill and W. Gray of CSU. The use of  $R$  stretches the radius of maximum wind by almost a factor of four. Using this tangential wind field we can easily determine the coefficients and the right hand side of (5.10). We have then used the multigrid methods of Brandt (1977, 1982) to solve (5.10) for  $\Psi^*$ . The resulting field of  $\frac{1}{\rho} \frac{\partial R\Psi^*}{R\partial R}$  is shown in Fig. 5. In this case deep convection

<sup>1</sup> For those so inclined, (5.12) could also serve as a basis of a hurricane modification theory.

reaching above 200 mb at  $R \sim 400$  km ( $r \sim 200$  km at  $p \sim 200$  mb) will be most efficient at converting total potential energy to kinetic energy.

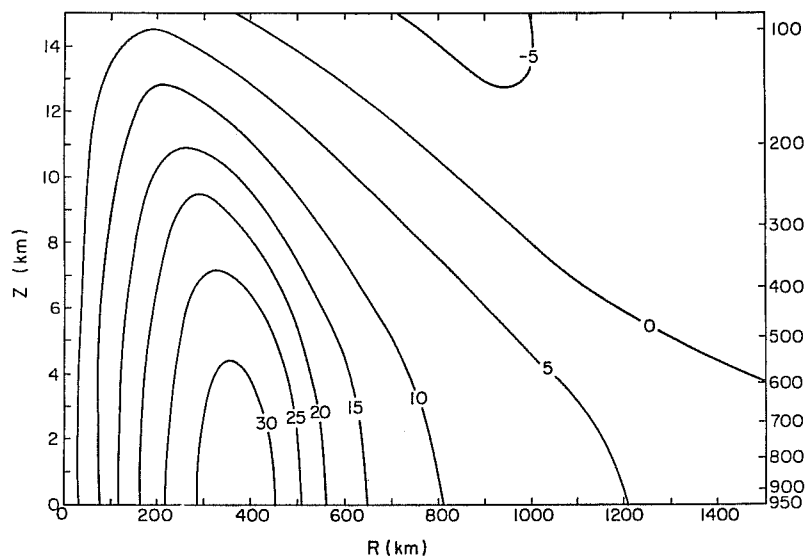


Fig. 4. The field  $v(R,Z)$  based on the large typhoon composite data of R. Merrill and W. Gray.

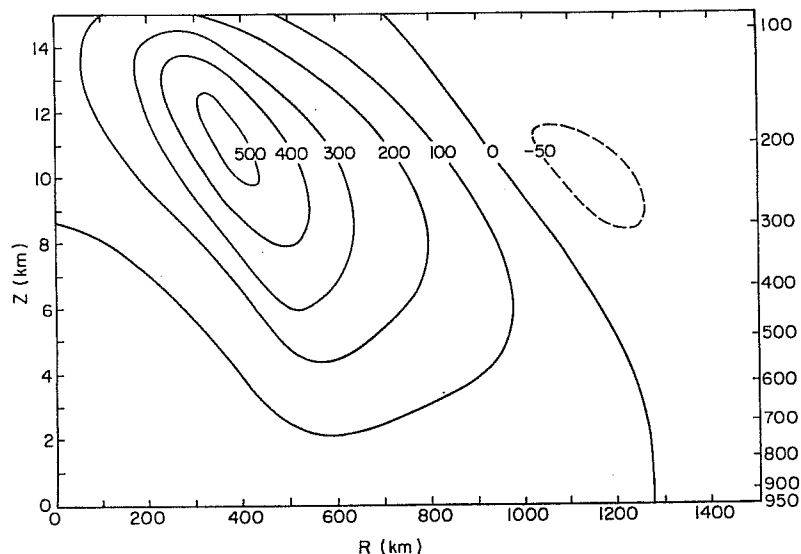


Fig. 5. Isolines of  $\frac{1}{\rho} \frac{\partial R\Psi^*}{\partial R}$  (meters). Large values indicate regions where convective heating  $Q$  would be most efficient at converting total potential energy to kinetic energy.

## 6. CONCLUDING REMARKS

The dynamical arguments given in this paper do not constitute a closed theory of hurricane development. Closed theories usually incorporate an equation (or system of equations) which relates  $Q$  to the other dependent variables of the model

(i.e. a cumulus parameterization). Unfortunately, there is no concensus on how this should be done. Indeed, it is not too much of an exaggeration to say that there are as many parameterization schemes as there are researchers in the field. However, in spite of the wide variety of ways that the "moist physics" has been treated in tropical cyclone models, there are certain common features to be seen in the output from such models. Among these common features is the nonlinear behavior illustrated in Figs. 1 and 2, and it is this behavior we have tried to understand with the Eliassen balanced vortex model.

#### ACKNOWLEDGMENTS

This research was supported by NSF Grant ATM-8207563. Development of the multigrid elliptic solver was supported by ONR Grant N00014-83-K-0068.

#### REFERENCES

- Brandt, A., 1977: Multi-level adaptive solutions to boundary-value problems. Math. Comput., 31, 333-390.
- Brandt, A., 1983: Guide to multigrid development. Multigrid Methods. (W. Hackbusch, U. Trottenberg, eds.). Lecture Notes in Mathematics, 960, Springer-Verlag, Berlin, pp. 220-312.
- Courant, R., and D. Hilbert, 1953: Methods of Mathematical Physics. Interscience Publishers Inc., New York.
- Eliassen, A., 1952: Slow thermally or frictionally controlled meridional circulation in a circular vortex. Astrophys. Norv., 5, 60 pp.
- Hack, J. J., and W. H. Schubert, 1980: The role of convective-scale processes in tropical cyclone development. Atmospheric Science Paper No. 330, Dept. of Atmospheric Science, Colorado State University, Fort Collins, CO, 206 pp.
- Hack, J. J., and W. H. Schubert, 1981: Lateral boundary conditions for tropical cyclone models. Mon. Wea. Rev., 109, 1404-1420.
- Hoskins, B. J., 1975: The geostrophic momentum approximation and the semi-geostrophic equations. J. Atmos. Sci., 32, 233-242.
- Hoskins, B. J., and I. Draghici, 1977: The forcing of ageostrophic motion according to the semi-geostrophic equations and in an isentropic coordinate model. J. Atmos. Sci., 34, 1859-1867.
- Schubert, W. H., and J. J. Hack, 1982: Inertial stability and tropical cyclone development. J. Atmos. Sci., 39, 1687-1697.
- Schubert, W. H., and J. J. Hack, 1983: Transformed Eliassen balanced vortex model. J. Atmos. Sci., 40, 1571-1583.
- Schubert, W. H., J. J. Hack, P. L. Silva Dias, and S. R. Fulton, 1980: Geostrophic adjustment in an axisymmetric vortex. J. Atmos. Sci., 37, 1464-1484.
- Silva Dias, P. L., W. H. Schubert and M. DeMaria, 1983: Large-scale response of the tropical atmosphere to transient convection. J. Atmos. Sci., 40, to appear in November issue.

Yanai, M., S. Esbersen and J.-H. Chu, 1973: Determination of bulk properties of tropical cloud clusters from large-scale heat and moisture budgets. J. Atmos. Sci., 30, 611-627.